

## Site selection, Measuring Instruments and Identification of Cloudy days

### 3.1 INTRODUCTION

Using the historical and meteorological average radiation database (of same frequency), some agencies have produced “Solar maps” for their respective countries. Standard plots to classify locations according to various climatic conditions are available. Hence, both these plots provide assistance in doing preliminary solar potential estimation and help in properly understanding the suitability of the location for any solar power plant installation. Now as discussed in the previous chapter, for any detailed analysis, ground station data is considered the most preferred one. Most of the solar power plants are located in a hot area, having dry conditions (barren areas). Hence, after detailed analysis of “Solar maps”, Jodhpur a city with “Hot and Dry” climate condition, located in the western part of Rajasthan, is selected and its ground-based radiation dataset is procured. This climate conditions naturally make this location unique for the study of detailed solar resource potential and are expected to help in setting up of any solar-based system. The presence of all types of climate conditions and maximum sunny clear-sky days make this location important. At Jodhpur, two independent solar radiation measurement stations are identified, possessing a similar type of solar radiation measuring instruments. For station comparison, the local condition details and instrument details are provided in this chapter. In this thesis, both stations are considered for data quality study and their measurement response from the radiation sensors for the same year are compared in later chapter. This process helps us in correction and modification of solar radiation database of the location.

Now while measuring the radiation parameters at the ground site, various types of error can occur. So, the way by which errors enter into the system is briefly discussed here in this chapter. Further, climate analysis is also studied, as for detailed radiation analysis both clear sky and cloudy days are to be considered.

### 3.2 SITE SELECTION AND LOCATION INFORMATION

Solar maps provided in literature [NREL, 2017; SolarGIS, 2017; IRENA, 2017; C-WET, 2017] for different parts of the world, help in the estimation of solar radiation potential of any desired location (see “Annexure A” for C-WET provided maps). These maps are prepared using historical 30-minute averaged satellite images and then compared with hourly averaged ground-based measured radiation database for its evaluation. Maps show contours in terms of yearly, monthly, daily and hourly radiation averages. A map of uncertainty (change in radiation over the years) is plotted by using previous years radiation database [C-WET, 2017]. Now in solar map analysis, one can see the highest GHI and DNI component measured in some portions of Northern, North-East, North-Western and South region of India. The reason behind these high values is that the location is at high altitude or near the tropic of cancer line. Any solar based power plant installed at these locations, will generate additional electricity as compared to other location. But the most favorable climatic condition is in North-West region. Here, vast barren land is available having good quantity of clear sky days. Whereas in other

regions, locations have mountains, waste-land is not available and have high climatic disturbances. However, the detailed radiation and climatic study of solar-rich potential sites in India, using high-frequency ground radiation database are still not carried out. Therefore in this research work, one location is selected and by using available radiation databases, its detailed analysis is done.

The north-western locations of Gujarat and Rajasthan are identified (using solar map) with good solar-rich potential locations. From which, "Jodhpur" is selected which is present at the western side of Rajasthan state. Further, for this location in-depth analysis is in high demand by solar power plant installers. This location is the second largest city in Rajasthan and is also popular with the name of "Sun City" [IMD (1) and IMD (2), 2015]. This state also has vast barren land with mostly sunny and clear sky condition days (around 300 days) throughout the year. Because of this, a significant number of solar based plants are being installed in Jodhpur and Jaisalmer regions. In addition, the presence of solar radiation measurement stations at the institute provides motivation in selecting this location. Hence one gets access to raw radiation database and live instrument responses which can be studied in detail.

In this study, standard solar radiation map provided by C-WET, (2017) is used to determine the long-term average of radiation values. Where, these map values are verified with genuine ground-based measured values and for the selected location, values given are GHI (5 kWh/m<sup>2</sup>/day) and DNI (5.35 kWh/m<sup>2</sup>/day). Hence, the site offers good radiation potential, and this location also has historical experience of having a high fraction of the beam component to the global radiation values [IMD (2), 2015]. Due to this, the temperature is extremely high (exceeds 40° C on any clear-sky days) between March to October, with an average temperature of 35.6° C (exception the monsoon period) [IMD (3), 2008]. The average rainfall is about 450 millimeters, which is less as compared to other solar-rich locations in India.

For checking climatic conditions: Köppen [Geiger, 1954] and MNRE [MNRE, 2006] classifications are used. Here for the selected location, climatic condition is identified by using MNRE, solar radiation handbook [MNRE, 2006]. For Indian locations this classification is suggested. In this classification, as given in Maxwell *et al.*, (1993) solar radiation database, climatic conditions and meteorological parameters for several locations can be obtained. Moreover, for location characterization, limits of temperature and vegetation limits are provided in tabular form, by which they divided the whole Indian continent into five climatic condition types [Bansal and Minke, 1988]. However, it was again refined by SP 7, (2005) and then finally four climatic zones are finalized. From which Jodhpur comes under "Hot and Dry" type climate location (for meteorological parameters limits and country map see Annexure B). Also, this location has vast barren lands which makes place eligible for any solar power plant installations. Now understanding the solar radiation data for this location can benefit in resource assessment of other locations, which have similar climatic conditions.

### **3.3 SOLAR RADIATION MEASUREMENT STATION AND ERRORS**

Two different independent agencies, located in Jodhpur, Rajasthan (India), measure solar radiation measurement values. The stations' names and locations are: SRRRA IIT-Jodhpur (26.27° N, 73.03° E) & IMD-Jodhpur (Agro) (26.25° N, 73.04° E). Both installations are near to each other (distance 2 Km, see Figure. 3.1) and the same instruments are used for solar radiation measurement. Hence, they both share the same climatic properties and data measured by them are comparable. The only differences between them are the installed location of the station and calibration/maintenance schedules. One is at the center of the city and other is located near agricultural land. Moreover, both stations strictly follow frequent cleaning and maintenance schedule, but still due to different location condition, variation in measurement values is seen.

Hence, the study of measuring instruments and identification of different measurement errors is required.

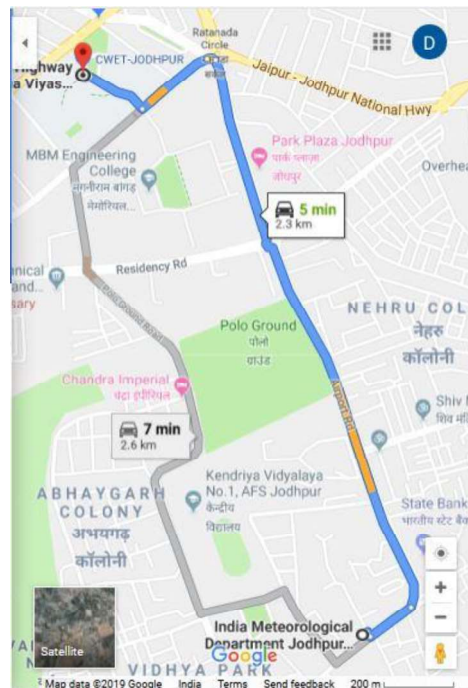


**Figure. 3.1:** Google Map showing the distance between IMD-Jodhpur (Lat. 26.25°N, Long. 73.04°E) and C-WET-Jodhpur (Lat. 26.27°N, Long. 73.03°E) (Source: Google Map)

### 3.3.1 Solar Radiation Station Measuring Instruments

For measuring different solar radiation components, measuring instruments with various sensing elements are used [Sukhatme and Nayak, 2008]. The latest sensors use dissimilar semiconductors or metals, which work on the principle of the Peltier effect. The most accurate and quick sensing sensors are thermopile based, here a group of thermocouples is arranged in a series or series-parallel to measure the increase in temperature at the black sensing plane. Now the heat generated at the thermopile plate is compensated by applying equivalent voltage on it, so that heat equilibrium is maintained [Kippzonen, 2017]. Hence, this equivalent voltage is converted into the desirable values of energy ( $W/m^2$ ). To get most accurate values from them, the sensor is protected from the base using hard support with proper heat sink arrangement and on top, quartz dome or window for correct measurement under high dynamic climate changing conditions [Duffie and Beckman, 2013].

In addition to the measurement of solar radiation values, each station also includes instruments for measurement of some related meteorological values. The frequency at which these values are measured is decided on the basis of instruments used. Usually, same frequency is maintained at which radiation values are measured. Among the instruments being operated at the selected location (Jodhpur, Rajasthan), all the solar radiation measuring instruments used are thermopile based and research grade instruments [ISO-9060, 2008 (see Annexure C)]. Use of first-class pyranometer and secondary standard pyrhemometers is suggested, at the ground-based installed solar radiation measurement station. Related meteorological parameters like wind speed, wind direction, air temperature, relative humidity, dew point and atmospheric pressure are controlled by WMO guidelines [WMO (2), 2008]. Typical weather and radiation station instrument list are provided in Table 3.1 [Kumar *et al.*, 2014].

The historical radiation databases usually have data available at either hourly or daily average values, but new stations measure values at high frequency (in minutes). Now while comparing the weather stations at our selected location, one finds that both stations measure radiation values at different intervals. IMD-Jodhpur measures at 1-minute interval and data available for analysis is of 10-minute interval. Whereas SRRRA-Jodhpur station measures all parameters at 1-second period and data provided for analysis is in a 1-minute interval. Moreover, in basic data examination, missing data problem is seen in both station databases. Hence both need data correction before performing any analysis.

**Table 3.1:** Type of Instruments, Model and Manufacturer Details Used in SRRRA stations [Kumar *et al.*, 2014]

Parameters	Type of Instruments	Model	Manufacturer
GHI	Pyranometer	PSP	Eppley Lab
DHI	Pyranometer	PSP	Eppley Lab
DNI	Pyrheliometer	NIP	Eppley Lab
-	Sun Tracker	SMT-3	Geonica
-	Data Logger	3000C	Geonica
Ambient Temperature and Humidity	Temperature and Humidity Sensor	41382VC	Young
Wind Speed and Direction	Ultrasonic Wind Sensor	85000	Young
Rain Accumulation	Rain Gauge	52203	Young
Barometric Pressure	Barometer	61302L	Young

### 3.3.2 Errors in Radiation Database

After the measurement of solar radiation values (available in the form of a database) its data verification is needed. Solar radiation measurement station installed at ground level is prone to measurement errors. Where these types of error can be classified into two groups: equipment and operation based errors [Younes *et al.*, 2005] and a list of all possible errors are provided in Table 3.2. Here occurrence of equipment based errors and uncertainties shows, the instrument is itself not performing well. This error needs quick correction, as faulty equipment don't give reliable values. The owner and installer of these instruments, should check these values and participate in regular calibration sessions to maintain equipment at desired measurement quality level. Now if the error is arising due to human or disturbed environmental conditions, then they come under operation related errors. These errors, which one identifies using specified relations can be corrected in some cases. Both these error classes need proper data (measurement feasibility) investigation before any correction is applied to it.

**Table 3.2:** Equipment and Operation Based Errors and Uncertainties

Equipment Errors & Uncertainty	Operation Related Problems & Errors
-Cosine Effect	-Dust, Snow, Dew, Water-Droplets, Bird Dropping, etc.
-Azimuth Error	-Incorrect Sensor Leveling
-Temperature Response	-Shading Caused by Building Structures
-Spectral Selectivity	-Electric Field in Vicinity of Cables
-Stability	-Mechanical Loading of Cables
-Non-Linearity	-Orientation and/or Improper Screening of the Vertical Sensors from Ground Reflected Radiations
-Complete or Partial Shade-Ring Misalignment	-Station Shutdown
-Dark Offset Long-wave Radiation Error	

For identification of these errors, making plots of the database and their transmittance ratios is the most common option [Younes *et al.*, 2005]. Here, for better understanding, each error response is identified at the clear-sky condition and discussed below with possible cause of its occurrence.

**(a) Cosine Effect**

Instrument sensor response at sunrise and sunset duration. Usually, the solar altitude of fewer than 6 degrees is ignored, because the optical error is high. Under this error, one can see the rapid drop in measured radiation values.

**(b) Azimuth Error**

This measurement error comes due to the presence of an optical loss in glass domes. Hence incoming radiation is not able to reach properly at the sensor and disturbing values are recorded. Hence during the installation of instruments and during maintenance schedules, their optical components and orientation need checking.

**(c) Temperature Response**

At station installed locations, whole day temperature variation also creates an error in the measurement process. To isolate the instrument from this error, the instrument is protected using double glass dome from the top and complete sealing from the back. Location where daily temperature range is varying (Deserts and snowfall areas), this error presence is possible. Nowadays, total environmental sealed instruments are coming, which don't get affected by this error.

**(d) Spectral Selectivity**

This error depends on spectral absorption of paint, spectral transmission of glass and factor determining deterioration of cells. As time passes the instrument quality degrades and values measured by them also reduces. The working sensor degrades at a rate of  $\pm 1\%$  change in full-scale measurement per year [Pape *et al.*, 2009].

**(e) Non-linearity**

This error occurrence is related to radiation received at the sensor plate. At high and low radiation conditions, the potential (eV) measured by the sensor, and its conversion to equivalent ( $W/m^2$ ) solar energy value, sometimes don't follow a linear relationship. It is an instrument related error and is controlled during the calibration process. However, its effect on total radiation values is relatively small.

**(f) Dark offset Longwave Radiation Error**

Due to sensor thermal imbalances, the measured values at night are recorded in the range of  $-5 W/m^2$  to  $-20 W/m^2$  [Stoffel and Reda, 2013]. Usually, if these values occur every night then instrument needs recalibration, and for occasional small intervals, it is corrected to zero values.

**(g) Complete or Partial Shade-Ring Misalignment**

Wrong instrument installation, missing tracking device or internal tracking algorithm problem are some reasons, due to which this error occurs. If identified, the GHI parameter is only accepted here, DHI and DNI component requires some investigation.

**(h) Dust**

In spite of daily cleaning, a small presence of dust is always seen deposited on the measuring instrument. If instruments are not cleaned regularly, then a regular decrease (lesser by 1 percent per day) is seen in GHI, DHI and DNI measurement value [Pape *et al.*, 2009]. Also, this dust presence affects in cloudy conditions days.

**(i) Dew and Water Droplets**

Water and water vapor presence on the inside and outside of instruments glass dome, don't allow full radiation to reach towards the sensor and all three radiation components are getting affected by it. The watermarks left after drying of water also reduces its radiation measuring ability.

**(j) Bird Droppings**

A common problem for station installed at any location. Bird droppings blocks openings of measurement sensors due to the presence of solid waste. Frequent cleaning is recommended for all measuring stations (it's the only solution). Here all three radiation parameters get affected due to this.

**(k) Incorrect Sensor Levelling**

Measured value when compared with solar angles, then this error is identified. If this pattern is repeating for a number of days, then it is labeled as incorrect sensor leveling. If leveling is correct, find some other valid reason for this variation. Hence GHI value can be reliable but DHI and DNI need some correction.

**(l) Shading by Buildings**

If every day for a specific period the measurement values drops, then the presence of some tree, building or any solid body presence is verified.

**(m) Electric Field Presence**

Presence of source of some high electric supply, makes the wire polarized and spikes in data can be easily seen in whole day radiation plot. If on all days (even any climatic condition), the presence of spikes is common, then this error is identified. This data can be directly corrected using some suggested data correction tool.

**(n) Mechanical Loading**

A similar pattern is seen like electrical field presence, but here reasons for the spikes are due to wire tension and occurrence of piezoelectric effect. Proper investigation is required as it reduces the life of the wirings.

**(o) Station Shutdown**

No data receiving from the station measurement sensors. Check the whole system for correct identification of no data receiving problem.

**3.3.3 Real Operational Problems**

Different errors discussed above are derived from a broad perspective, and its identification is seen only for clear sky days. Now some real-life problems identified while running the plants are discussed below. These problems are identified and concluded after observation of 51 SRRA stations, 2011-2012 radiation database [Kumar *et al.*, 2014].

**(a) Weathering of Solar Radiation Sensors**

The sensitivity of sensor reduces after some period of operation, hence periodic calibration of instruments is suggested. Also, the surrounding condition present at the location seasons the system and it degrades measurement process.

**(b) Soiling of Sensors**

Presence of dust and soil near measurement station gets settled on the measurement sensor and doesn't allow full radiation to reach the sensor. Daily cleaning of the sensor is recommended, but total removal is not possible. Dust present in the atmosphere always makes

a small thickness of dust on it. A standard range is also provided in data quality checking guidelines, but after that cleaning is required.

**(c) Bird Hit**

It's a serious problem related to the life of measuring instruments. Birds usually hit the ultrasonic wind sensor and other sensors (also tries to sit over it). Protection cages are also installed near the sensor, but full success is still not achieved. Birds chewing the instrument connecting wires is also seen in some of the stations.

**(d) Changing of Site Exposure Conditions**

In the surroundings of the station, every year proper cutting of trees-bushes and shrubs are required. Otherwise, they may shade the sensor and values measured by this sensor are found incorrect. However, proper cleaning is required if the station is located near some industry or chemical processing unit.

**(e) Vandalism of Equipment**

Some stations established in "Indian Solar Mission" reported missing of battery and solar panels, due to no security presence at that location. Now all stations are placed at some height on the building with security, so now no cases of theft are reported and good quality radiation data is received by them.

Some other reasons of error occurrence are the inaccessibility of the plant, data failure while transmission, equipment failure and uncontrollable data gaps in the database. Identifying them in the measured database is difficult, as at single time interval, multiple errors are possible.

### **3.4 RADIATION MEASUREMENT ERROR IDENTIFICATION APPROACHES**

Literature provides some approaches, by which one can identify errors (listed above) in the solar radiation database. Hence, in this process transmittance ratios are used and then for error identification, its comparison is done with Maxwell *et al.*, (1993) plots and relations.

#### **3.4.1 Using $k_t$ - $k_n$ Plots**

According to Maxwell *et al.*, (1993), a simple " $k_t$ - $k_n$ " plot can easily predict various climatic conditions of the site. Maxwell *et al.*, (1993) suggested a standard plot, which clearly identifies each climatic condition (see, Figure 2.2). Now in transmittance ( $k_t$ - $k_n$  and  $k_t$ - $k$ ) plots, any data which goes outside the suggested plot or shifts with time helps us to identify errors in the database. Here used transmittance factors and their ratios are described in the previous chapter and details can be seen in Table 2.4. Moving forward, Younes *et al.*, (2005) have used this dataset and by taking Bahrain, 5-min averaged data (28 March-30 September 2000) its climate results in " $k_t$ - $k_n$ " plot is studied. For identification of errors in the database, here " $k_t$ " values are divided into n-bands and for each " $k$ " band, specific mean and the standard deviation is calculated. Using these values of transmittance ratios, acceptable lower and upper boundaries are defined. Where data falling outside these boundaries need to be analyzed and the constant trend is identified for error identification.

From the IMD-Jodhpur database, one-month data (February-2015, 10-Minute interval) is analyzed by plotting its " $k_t$ - $k_n$ " characteristics (see Figure 3.2). This plot is directly compared with plots provided by Maxwell *et al.*, (1993) and Younes *et al.*, (2005). The analysis shows operation related error with some days having a shade-ring misalignment. Now for further detailed analysis, some additional plots and their inter-comparisons are used as discussed below:

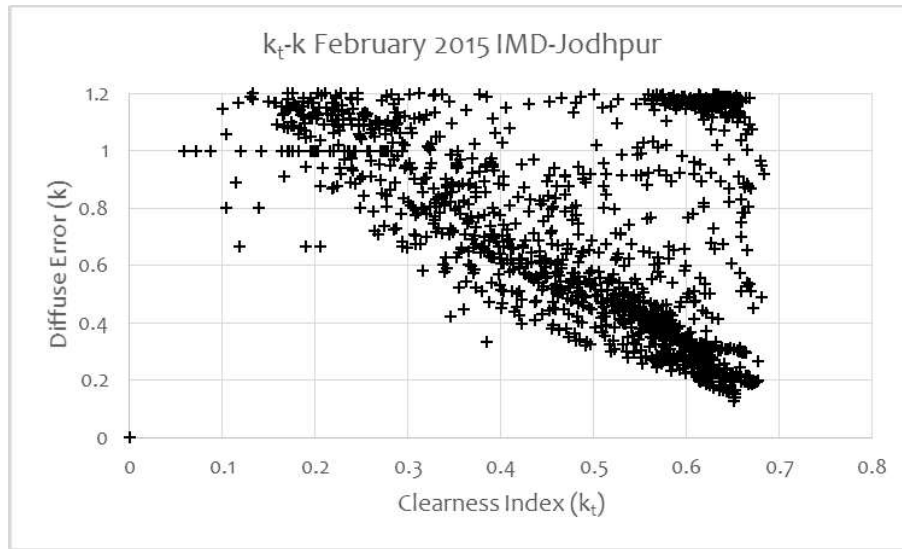


**Figure 3.2:**  $k_t$ - $k$  Plot for IMD-Jodhpur, 10-min Averaged Data for (01-28) February 2015

### 3.4.2 Using $k_t - k_n$ and $k_t - k$ Approach

Selecting two radiation databases at nearby locations, their " $k_t - k_n$ " and " $k_t - k$ " plots are drawn and results according to instrument measurement quality are compared [Journée and Bertrand, 2011]. During the analysis, investigating the correctly measured radiation component is difficult; hence the comparison is done between reliable instruments and deficient instruments by using the measured database and the simulated dataset. Moreover, a climatological quality envelope is also suggested, derived from historically available previous two years (2008 and 2009) quality tested data. The range finalized for this envelope, can check everyday transmittance ratios for their specific location (erroneous data can be identified). Using " $k_t - k$ " plot, one has also identified, calibration error due to global and direct radiation component using two different stations (two-month dataset).

### 3.4.3 Using Theoretical and Actual GHI Measured Values

Another method to check data quality is to compare theoretically calculated GHI with actual measured GHI values recorded from the instruments [Tejera *et al.*, 2015]. Here for measured radiation data analysis, 4 radiation measurement stations at different environmental conditions and recording intervals are used. As for a well-maintained station (on clear sky day), for the ratio of measured and calculated GHI value the majority of data should consistently fall in a straight diagonal line with a slope of 45 degrees. Now available solar radiation components (DHI and DNI) are identified and theoretical GHI is calculated from it. After a comparison of this calculated GHI with an actual measurement, errors are identified. Some cases in these analysis errors due to dust, instrument offset, and change in recording frequency, timestamp error and tracker alignment error are identified.

Using these calculated and measured GHI plots, other climatic events can be studied to differentiate the response of the instrument under different error conditions. Due to the dust on sensor conditions, all radiation components get affected and by visual inspection of all radiation components for nearby days, one can ascertain its presence. Physical identification in GHI scatter plot is slight difficult due to scattering of data points at lower and mid portion. In offsets error identification, the instruments measure values below  $-4$  ( $W/m^2$ ) or above  $50$  ( $W/m^2$ ) in the night time. Literature shows the procedure to correct these values in the night time, but data



measured in the daytime may be unreliable. Now in the visual identification of both plots, independent lines of different orientations is seen.

A change in recording frequency means either the value is not measured at that specified interval or data is saved at an incorrect time interval. Hence the scatter plot shows non-uniform plotting and its area is broad due to averaging issues. Another similar case is the presence of timestamp error. Sometimes due to different time zones or wrong coordinates input in the data logger machine, the data is not able to get stored at the correct time stamp. Here the scatter plot will be uniformly spread and no coherence is seen between the radiation components. In tracker alignment error, only the GHI component is found useful and other components are found erroneous. The slope in the GHI scatter plot indicates it is also of no use as two radiation components are found faulty in visual analysis.

Here all these processes of error identification are analyzed for a one-year radiation database, in an efficient manner. The conditions in which these errors are identified are described in detail above. The correction procedure at the high measurement frequency is not discussed so far in the literature. Hence, one has to look at the individual measured interval and error identification and correction is done.

### **3.5 IDENTIFICATION OF DAYS ACCORDING TO CLOUD CLASSIFICATION**

Every day is not a clear sky day, and characterizing each day with respect to cloud condition is possible. Similarly, the occurrence of a cloudy day (even with other measurement errors) is possible. Hence, differentiation of both types of the condition is important, as one is working at high-frequency values (1-second to 1-min measured values). Moreover, throughout the year, identification of absolute clear sky days is uncommon. Jodhpur has large number of clear sky days in Rajasthan. The conditions which help in the classification of various cloudy condition days are discussed in detail below. After that from Jodhpur radiation database, different cloud condition days are identified, and their corresponding plots are discussed.

#### **3.5.1 Cloud Classification Guidelines**

For theoretical determination of solar radiation on all days of the year, one has to study various cloud parameters (droplet size distribution, cloud density, thickness, altitude, and temperature profile, etc.). As cloud can be considered as an aerosol layer composed of water molecules (liquid and frozen form) with gas particles. Instruments are involved for measuring these values, and heat-transfer equations are needed for actual radiation value estimations. Moreover, approaches used to identify different cloud conditions are typically divided into the following groups:

- i) Direct Visual Analysis (per Hour, Operators Check Cloud Presence in the Sky Manually)
- ii) Instruments using Doppler or IR sensors (which Senses Height and Volume of Cloud)
- iii) Using Cloud Images (received from Sky or ground-based camera)
- iv) Information Gathering using Radiation Measured at the Ground Measurement Station.

In old times because of non-availability of good quality sensors for cloud classification, its presence in the sky is measured and recorded manually by the operator himself. One has to go outside at the measuring site; analytically cloud presence is measured in terms of "oktas". Next accurate approach is by obtaining pictures of Earth's climate surface from the satellite and image is analyzed for the percentage of cloud presence in the sky. Now from the available sky image, its negative image is produced, which highlights bright portions of the image and cloud

presence is identified. Higher the transparency in this processed image, higher the possible chances of thick clouds. Moreover, if the image is processed with uniform time-step, then cloud motion and construction information can also be extracted from these series of pictures. Also by using satellite images and data processed after its image analysis, cloud and weather analysis can be done for any location [Reno and Stein, 2013]. When combining them with ground-based imaging and observation systems using TSI, Doppler or sky camera, they can detect all types of clouds. The radiation data measured here are accurate and helpful for specific plant analysis [Heinle *et al.*, 2010]. All methods used in cloud analysis utilizing various imaging devices and sensors, its processing approach are discussed in details by Tapakis and Charalambides, (2014). Due to non-availability of sky images for Jodhpur, this approach is not discussed in detail.

Sometimes historical sky images and other cloud-related meteorological parameters are not available. Now if ground-based hourly or sub-hourly measured radiation dataset is available, then plotting it helps in identifying the climatic condition. Hence in this research, for identification of various clouds, transmittance ratio plots are used. Transmittance values are calculated by using the ratios of measured solar radiation with theoretical maximum measurement possible. Literature [Geuder *et al.*, 2015] shows three transmittance ratios, discussed in the previous chapter. Moreover, a modified clearness index is also proposed [Sánchez *et al.*, 2011], where one needs daily averaged turbidity and calculated air-mass values (for that location) (see Eq.(3.1)). For calculation of Linke turbidity, guidelines given by Page, (1961) and Muneer, (2004) are followed. For air mass calculation, solar angles are calculated, according to the time of day.

$$k_t' = \frac{k_t}{1.031 \left( \exp \left( \frac{-T_L}{0.9 + \frac{9.4}{m}} \right) \right) + 0.1} \quad (3.1)$$

Now modified cloud classification is done according to Sánchez *et al.*, (2011); Perez *et al.*, (1992), by using modified clearness index ratios for different cloud types (see Table 3.3). But the suggested guideline is 0.3-0.7, therefore approaches for cloud condition can be re-classified in four classes. Now the partial cloud condition is divided into two parts, whereas clear sky and heavy cloud condition days are not disturbed. The motive behind this change is to see the variation in radiation measurement with constant light cloud and small-medium cloud present in the open sky.

**Table 3.3:** Different Cloud Conditions, Modified Clear sky and Direct Transmission Ratios

Cloud Conditions	$k_t'$ (Modified $k_t$ ) [Sánchez <i>et al.</i> , 2011]	$k_n$ (Direct Transmittance) [Maxwell <i>et al.</i> , 1993]	$k_t$ (Clear Sky Ratio) [Iqbal, 1983]
Clear Sky	Greater than 0.7	0.55-0.43	0.9-0.7
Partial Clouds	0.7-0.4	0.42-0.25	0.7-0.3
Heavy Clouds	Less than 0.4	0.24-0.16	0.0-0.3

**Table 3.4:** Different Cloud Conditions, Modified Clear sky and Direct Transmission Ratios (Modified)

Cloud Conditions	$k_t$	$k_n$
Clear Sky	Greater than 0.7	0.55-0.43
Light clouds	0.7-0.63	0.42-0.34
Medium Clouds	0.63-0.5	0.33-0.25
Heavy Clouds	Less than 0.5	0.24-0.16

These unit-less limits provided by Maxwell *et al.*, (1993) and SERI-QC, can identify various types of cloud condition days (see Fig. 2.1). Now see Table 3.3, for the understanding of this plot, where values are converted into a tabular form and used as sky and ground imaging approach [Chico *et al.*, 2011]. Another modified cloud classification approach uses modified clear sky coefficients (see Table 3.4). Using Eq. 3.1, these modified values are calculated and they are inter-related with direct transmittance ratio at different cloud conditions. For final verification of this cloud conditions and transmittance ratio values, different climate conditions are extracted from the available radiation database. Here each day is studied using listed cloud classification plots.

### **3.5.2 Cloud Condition Days and Respective Instruments Response**

Measurement response of each instrument at different cloud conditions is studied here. This task is essential, as measured data may contain a mixture of errors due to cloud presence and instrument/operation based errors. Independent identification of both error cases is required, and after that accurate guideline can be created for solar data corrections. Now from the location radiation database, different cloud condition days are identified carefully (these days should be free from all instrument/operation based errors). The climatic days and their response to various measuring instruments are discussed by NOAA, (2017). For proper identification of different climatic condition days, one can compare measured values with any standard clear sky model or ideal cloudless day or comparison of ideal day length with measured sunshine hours for each day. Some results in this direction are shown below.

#### **(a) Clear Sky Day (or Sunny Day)**

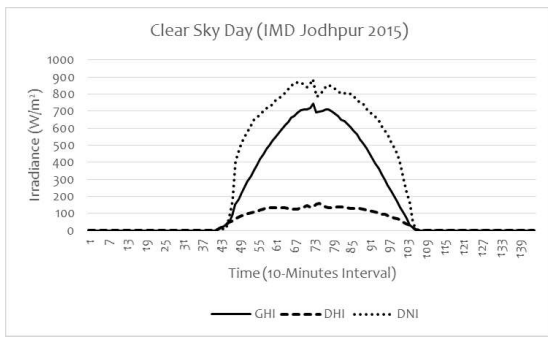
Any day having less than 10% cloud presence is considered as a clear sky day. From the available database, 27 January 2015 is found to be nearly comparable with theoretical clear sky day. Hence under these days, generated transmittance plots ( $k_t$ - $k_n$  and  $k_t$ - $k$ ) show similarity according to the present plot. Also the ratio of the theoretical model and measured GHI values fall in similarity range of 90-95%. Here radiation plots and transmittance plots look smooth with fewer variations (see Figure 3.3).

#### **(b) Passing and Scattered Cloud Day**

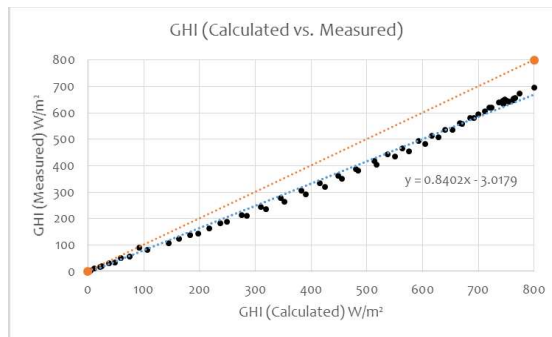
There is always some cloud present in the sky, either stationary (scattered cloud) or moving (passing cloud). From the available database, on 10 January 2015, the day is identified as clear-sky day with some clouds. Cloud size present, its motion and its transparency affect the sunlight coming on the Earth's surface. Hence for identifying these types of days, ( $k_t$ - $k_n$  and  $k_t$ - $k$ ) plots are used. These show a decrease in clearness index and transmittance ratio (when compared with standard transmittance plot of Maxwell) (see Figure 3.4). Measured-modeled GHI plot shows the similar result as clear sky day.

#### **(c) Haze Sky Day**

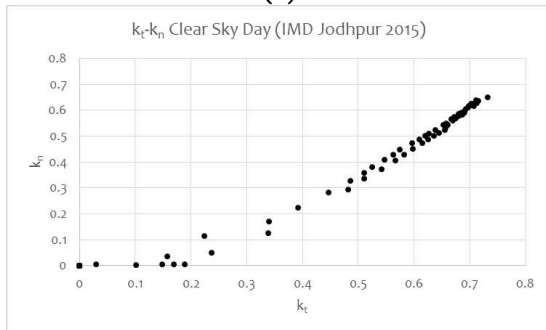
On these types of days, one can observe the constant presence of a uniform layer of cloud or aerosol present on the Earth's climate. Due to which GHI and DNI are reduced, and DHI value gets increased. On 2 January 2015, there is a uniform thin layer of rain clouds present. All three radiation components are correlated with each other, but in transmittance plots, one can see further decrease in maximum value of " $k_t$ " and " $k_n$ " correlation values, whereas " $k$ " value increases (see Fig. 3.5).



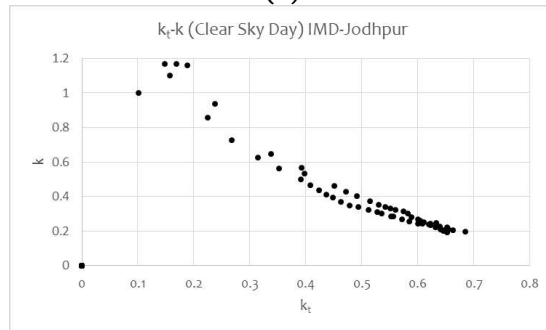
(a)



(b)

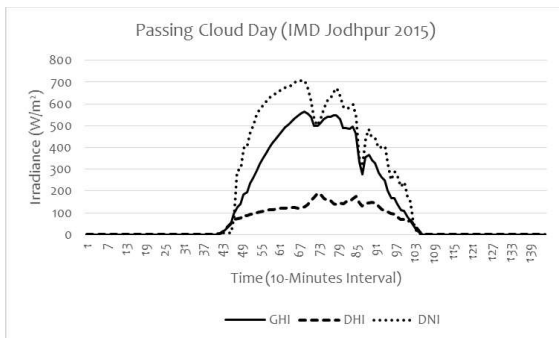


(c)

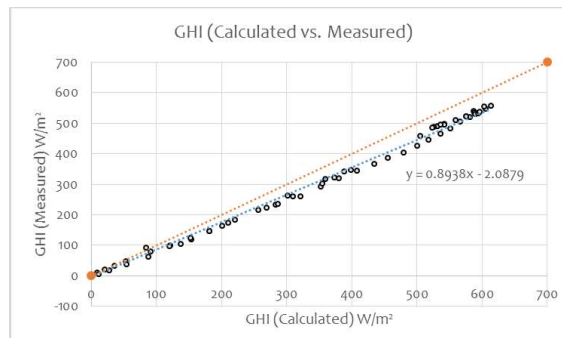


(d)

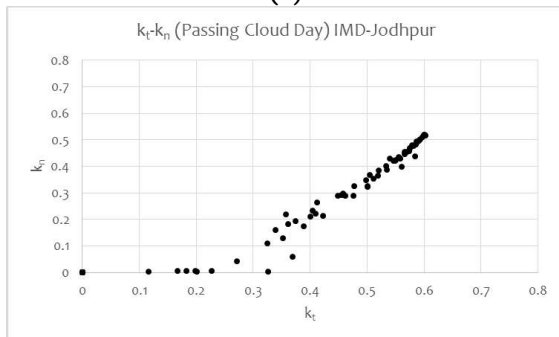
**Figure 3.3:** (a) Radiation Components (b) GHI (Calculated vs. Measured) (c)  $k_t$ - $k_n$  Scatter Plot and (d)  $k_t$ - $k$  Scatter Plot (Clear Sky Day, 10- Minute Interval Database, 2015, IMD-Jodhpur)



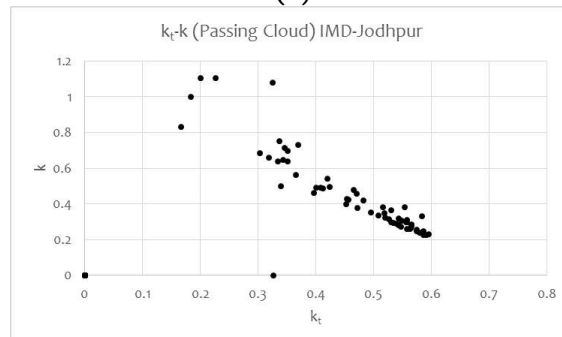
(a)



(b)



(c)



(d)

**Figure 3.4:** (a) Radiation Components (b) GHI (Calculated vs. Measured) (c)  $k_t$ - $k_n$  Scatter Plot and (d)  $k_t$ - $k$  Scatter Plot (Passing Sky Day, 10- Minute Interval Database, 2015, IMD-Jodhpur)

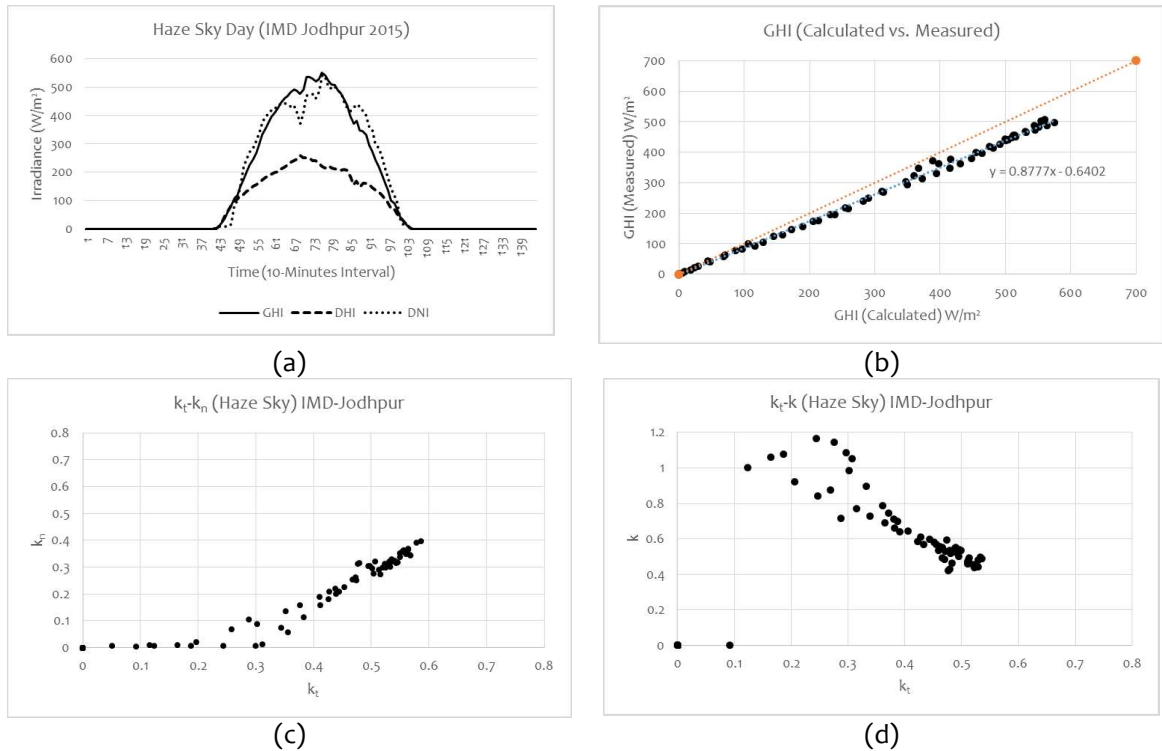


**Figure 3.5:** (a) Radiation Components (b) GHI (Calculated vs. Measured) (c)  $k_t-k_n$  Scatter Plot and (d)  $k_t-k$  Scatter Plot (Haze Sky Day, 10- Minute Interval Database, 2015, IMD-Jodhpur)

**(d) Partly Clouded Sky**

These days come under cloudy condition days, where cloud presence in the sky can be characterized between 2/8th and 6/8th (oktas) of the sky is covered. These days are also known as half cloud cover day and some interval of sunshine presence is seen. Here for the day selected (1 January 2015), one can see heavy cloud presence during morning and evening and during noon passing cloud, conditions are identified (see Figure 3.6). Due to which decrease in “ $k_t$ ” and “ $k_n$ ” values and increase in “ $k$ ” values is seen (as compared with clear-sky). Here measured-modeled GHI plot shows symmetry between them.

**(e) Broken clouded Sky**

This type of cloud-climate condition has heavy cloud presence (which covers between 5/8ths and 7/8ths of the sky) with no rain and sunshine. Here for the day selected (1 August 2015), both GHI and DHI measured components look alike, and measured DNI value is nearly zero. Here in transmittance plot, one can see all data is lying on one of their axes (verified with Maxwell *et al.*, (1993)) and measured-modeled GHI plot, shows symmetry between them (see Figure 3.7).

**(f) Thunderstorm Day**

A storm of lightning and thunder produced by a heavy structure cloud, usually producing gusty winds, heavy rain and sometimes hail. This selected day (12 August 2015) is similar to broken cloud day, but the difference is the additional presence of heavy rain (verification from available climatic data). The identification of these types of days can be made by seeing a sudden drop in GHI and DHI value (nearly zero) for that rain interval. This drop shows presence of water (due to rain) on radiation measurement sensors with no sunshine. Here the basic radiation and transmittance plots look the same as broken cloud condition days (see Fig. 3.8).

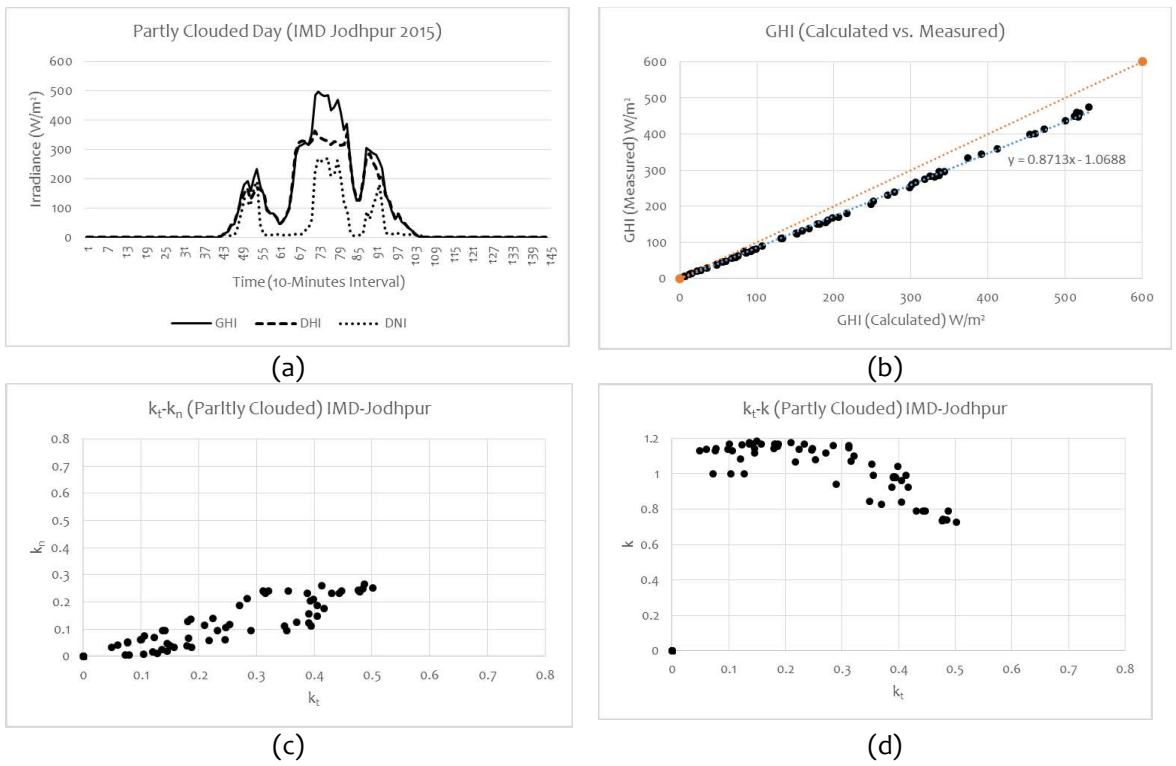


**Figure 3.6:** (a) Radiation Components (b) GHI (Calculated vs. Measured) (c)  $k_t$ - $k_n$  Scatter Plot and (d)  $k_t$ - $k$  Scatter Plot (Partly Clouded Sky Day, 10- Minute Interval Database, 2015, IMD-Jodhpur)

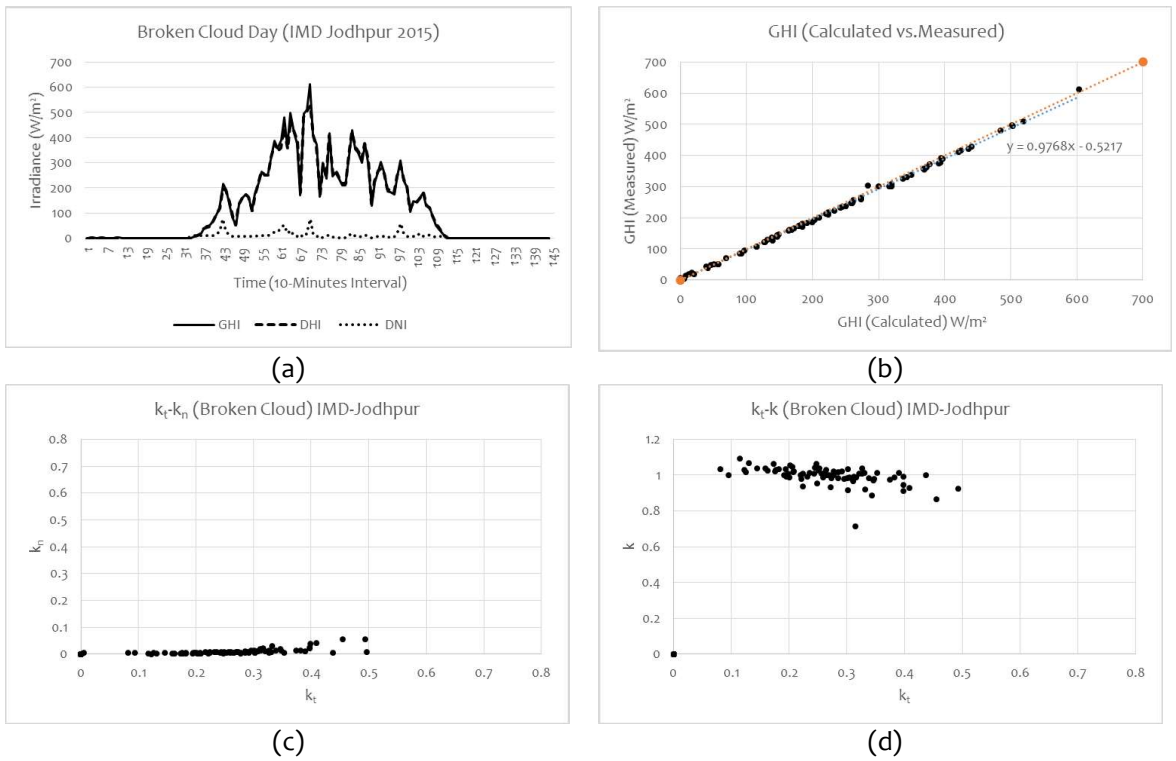


**Figure 3.7:** (a) Radiation Components (b) GHI (Calculated vs. Measured) (c)  $k_t$ - $k_n$  Scatter Plot and (d)  $k_t$ - $k$  Scatter Plot (Broken Clouded Sky Day, 10- Minute Interval Database, 2015, IMD-Jodhpur)

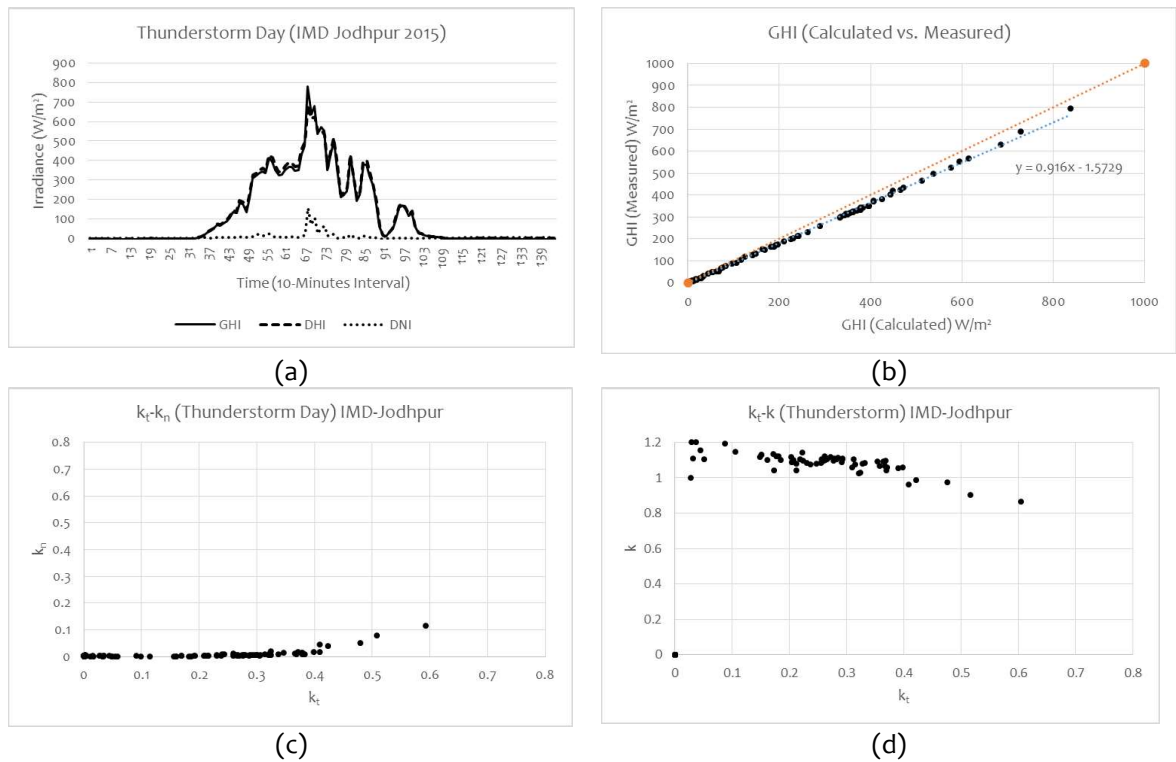


**Figure 3.8:** (a) Radiation Components (b) GHI (Calculated vs. Measured) (c)  $k_t$ - $k_n$  Scatter Plot and (d)  $k_t$ -k Scatter Plot (Thunderstorm Day, 10- Minute Interval Database, 2015, IMD-Jodhpur)

**(g) Drizzle Day**

This climatic condition is classified as day having heavy cloud presence with regular rainfall of small and slowly falling water droplets of diameters between 0.2 and 0.5 millimeters. On 31 July 2015, it looks like broken cloud day, but with using an additional meteorological database, the presence of 0.1mm rainfall for a repeated period of time is found on that day. One can see high measured values of GHI and DHI values and less presence of DNI values. The reason behind this is the presence of heavy moisture (presence of small interval rainfall) and cloud presence on this day. The transmittance plot also identifies the presence of a heavy cloud (see Fig. 3.9).

**(h) Sandstorm Day**

Climatic day identified as dust storm day is present, when high surface winds have picked up loose dust, which reduces the visibility to less than a one-half mile. Now 20 May 2015 is identified as having a sandstorm event and is verified due to the visible shifting of radiation measurement values without any reason. The generated " $k_t$ - $k_n$ " plot, shows lots of similarities between haze type and duststorm days. But the measured value of both days varies. Measured GHI and DHI value show the impression of a clear sky day, but a shift in DNI component indicates changes in the climatic condition. Here due to the combined presence of the wind and sand-storm, this DNI radiation pattern is possible (see Fig. 3.10).

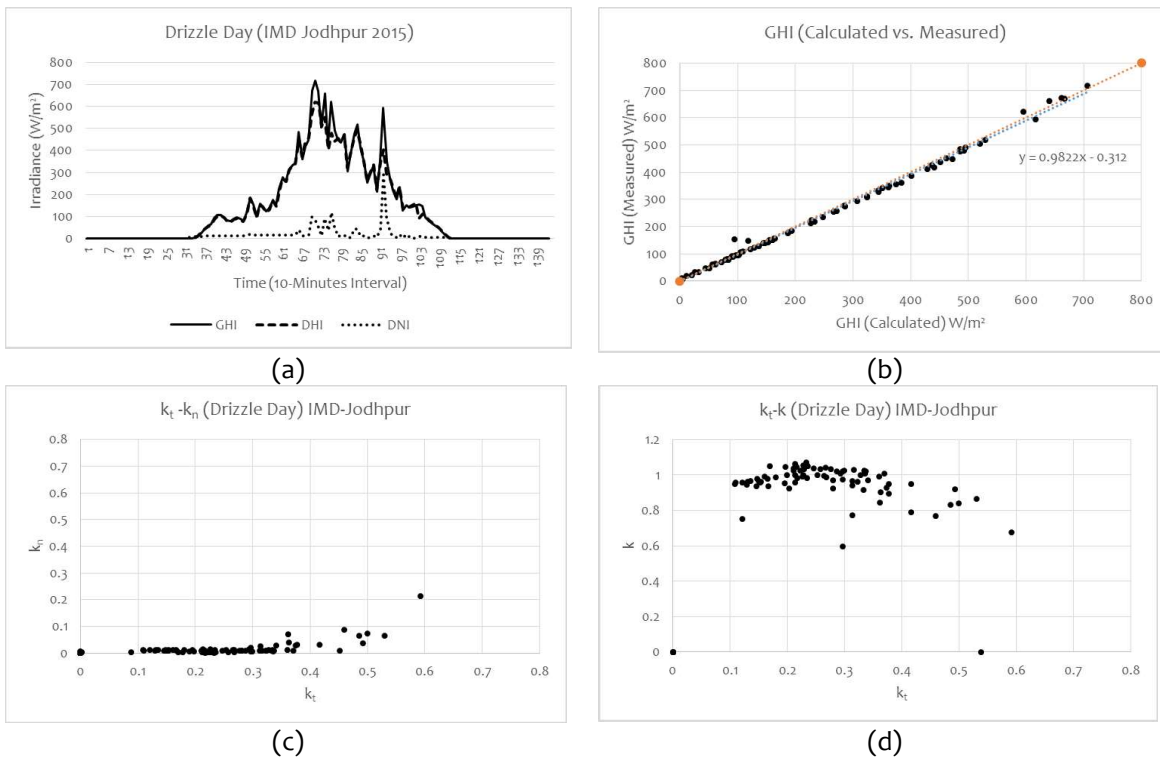


**Figure 3.9:** (a) Radiation Components (b) GHI (Calculated vs. Measured) (c)  $k_t - k_n$  Scatter Plot and (d)  $k_t - k$  Scatter Plot (Drizzle Day, 10- Minute Interval Database, 2015, IMD-Jodhpur)

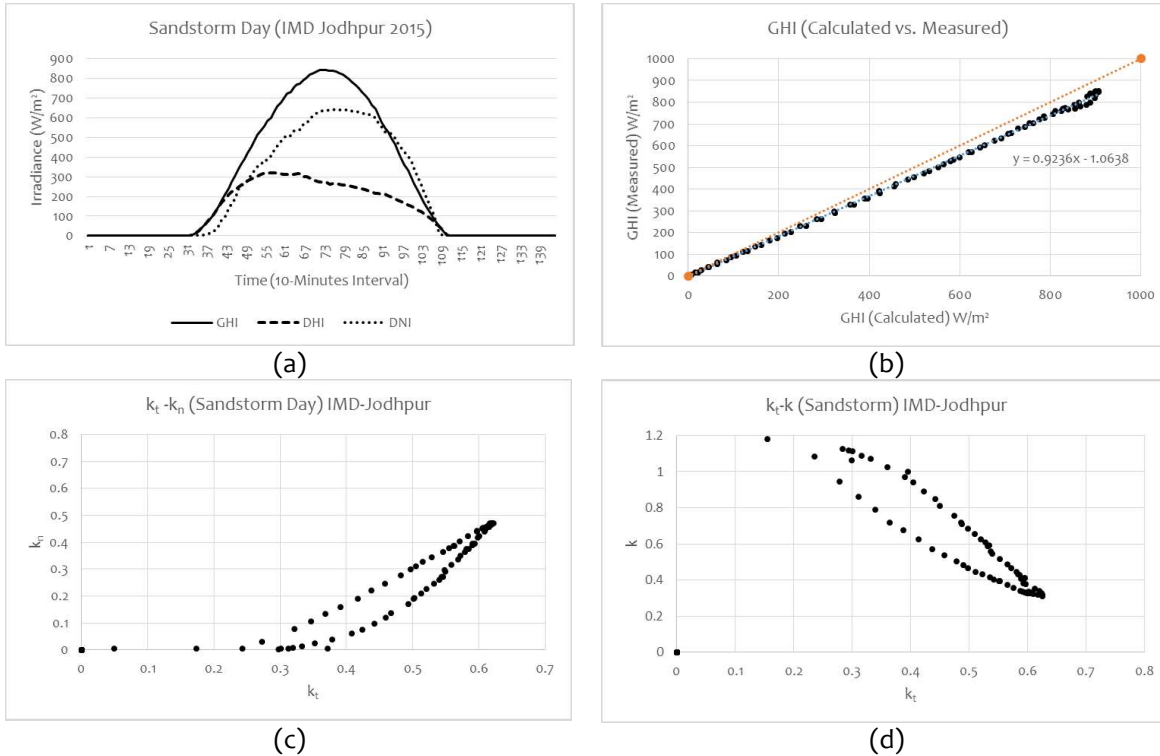


**Figure 3.10:** (a) Radiation Components (b) GHI (Calculated vs. Measured) (c)  $k_t - k_n$  Scatter Plot and (d)  $k_t - k$  Scatter Plot (Sandstorm Day, 10- Minute Interval Database, 2015, IMD-Jodhpur)



### 3.6 SUMMARY

Using a solar map provided by various sources, all solar rich potential locations for “India” can be identified. Out of which the location selected (Jodhpur, Rajasthan) is gifted with highest clear sky days and having vast barren lands, which attract large solar based plant installers. In addition at this location, two radiation stations exist for which raw radiation database is available, with access to measuring instruments. Now for this location, climatic and installed instruments study (sensing quality and measuring frequency) is done, with specific emphasis on errors (instrumental and operation based) occurred during the radiation measurement process. Some real-life errors are also discussed, which are reported by different plant owners. Basically, the radiation falling on any location is mostly affected by climate conditions and plant operating conditions. Individual identification of both these cases is primary, an error due to cloud presence requires no correction but for operation based, correction is required. Hence in this chapter, one has used plotting of different transmittance ratios and theoretical-calculated GHI methods to identify different climatic conditions. Now different cloud condition days are identified from the available radiation database and their responses are discussed for its characterization. In the following chapter, identification of operation based errors will be discussed at different cloud condition days.

...

